A new level set model for cell image segmentation*

Ma Jing-Feng(马竞锋)[a], Hou Kai(侯 凯)[c],
Bao Shang-Lian(包尚联)[b][c], and Chen Chun(陈 纯)[a]†

[a] *College of Computer Science and Technology, Zhejiang University, Hangzhou* 310027, *China*
[b] *Beijing Key Lab of Medical Physics and Engineering, Peking University, Beijing* 100871, *China*
[c] *Beijing Healthway Technology Limited Company, Beijing* 100084, *China*

(Received 23 August 2010; revised manuscript received 21 September 2010)

In this paper we first determine three phases of cell images: background, cytoplasm and nucleolus according to the general physical characteristics of cell images, and then develop a variational model, based on these characteristics, to segment nucleolus and cytoplasm from their relatively complicated backgrounds. In the meantime, the preprocessing obtained information of cell images using the OTSU algorithm is used to initialize the level set function in the model, which can speed up the segmentation and present satisfactory results in cell image processing.

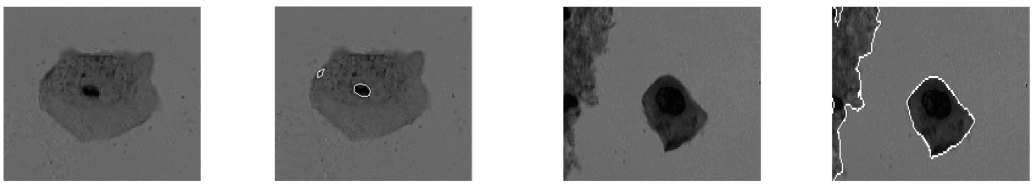
Keywords: cell image segmentation, 3-phase, level set, OTSU algorithm

PACS: 87.57.nm **DOI:** 10.1088/1674-1056/20/2/028701

1. Introduction

Since Lian *et al.*[1] published a paper dealing with cervical carcinoma cell images, cellular pathology has become an important research subject for tumor diagnosis and treatment. How to effectively and efficiently segment the nucleolus and the cytoplasm from their backgrounds is of much significance and many algorithms have been developed to achieve this goal over the past decades.

Traditional methods such as the pixel-based method, the edge-based method and the continuity-base method have relatively fast execution.[2] However, when the images are relatively complicated, it is often difficult to present good results. The active contour model[3−5] dependent on variational function[6] is a type of segmentation method that has been rapidly developed recently. It can be easily implemented in an energy minimization framework and in this framework a priori knowledge of shape and intensity can easily be included.[7] Active contour models are often divided into two main subclasses: edge-based models[8−12] and region-based models.[4,5,13−18] Li[7] and other investigators[19−21] proposed a region-scalable fitting energy model to solve the problem of inhomogeneous intensity. These methods perform well in segmenting MRI images, but when we apply them to cell image segmentation, we find that speed is slow when the image size is large and the result is greatly dependent on the initial setting of the level set function. For example, the segmentation result often converges to a local optimal solution if the initial level set function is not set appropriately, as shown in Fig. 1.



(a) (b) (c) (d)

Fig. 1. Cell images: (a) original image; (b) segmented image using a previous method, in which the cytoplasm has not been segmented appropriately; (c) original image; (d) segmented image using traditional level set method, in which the nucleoli has not been segmented appropriately.

*Project supported by the National Basic Research Program of China (Grant No. 2011CB707701), the National Natural Science Foundation of China (Grant No. 60873124), the Joint Research Foundation of Beijing Education Committee (Grant No. JD100010607), the International Science and Technology Supporting Programme (Grant No. 2008BAH26B00), and the Zhejiang Service Robot Key Laboratory (Grant No. 2008E10004).

†Corresponding author. E-mail: chenc@cs.zju.edu.cn

© 2011 Chinese Physical Society and IOP Publishing Ltd

In the present article, the special structure of the cell is utilized, we use the traditional pixel-based method to achieve the estimated original intensity of the nucleolus and cytoplasm to initialize the level set function. In our experiments, we can not only speed up the segmentation, but we are also more likely to obtain the global optimal solution.

2. Method of cell image segmentation

2.1. Region-based active contour model

Let $\Omega \subset R^2$ be the image domain and $I : \Omega \to R$ a given gray level image. In Ref. [6], the image segmentation problem was formulated by Zhao as follows: given an image I, find a contour C which segments the image into nonoverlapping regions. The following energy functional was proposed:

$$\mathscr{F}^{\mathrm{MS}}(u, C) = \int_{\Omega} (u - I)^2 \mathrm{d}x + \mu \int_{\Omega \backslash C} |\nabla u|^2 \, \mathrm{d}x + \upsilon \, |C| \,, \quad (1)$$

where u is an approximation of the original image, the approximation image is smooth within each of the connected components in the image domain Ω separated by the contour C ; $|\nabla u|$ represents the gradient of u; $|C|$ is the length of the contour C; $\Omega \backslash C$ is the area of Ω that excludes C; μ and υ are two coefficients of the relevant parts. In practice, it is difficult to minimize functional (1) due to the unknown contour C of the lower dimension and the nonconvexity of the functional.

Chan and Vese[4] proposed an active contour approach to the MS problem for a special case where the image u in functional (1) is a piecewise constant function. For an image I, they proposed to minimize the following functional:

$$\mathscr{F}^{\mathrm{PC}}(C, c_1, c_2) = \lambda_1 \int_{\mathrm{outside}(C)} (I - c_1)^2 \mathrm{d}x + \lambda_2 \times \int_{\mathrm{inside}(C)} (I - c_2)^2 \mathrm{d}x + \upsilon \, |C| \,, \quad (2)$$

where outside(C) and inside(C) are the regions outside and inside the contour C, and c_1 and c_2 represent two constants that approximate the image intensities in outside(C) and inside(C), and λ_1, λ_2 and υ are the relative coefficients again.

In Ref. [7], Li proposed a region-scalable fitting energy functional which makes the model handle the inhomogeneous intensity and speeds up the segmentation process. The proposed functional is as follows:

$$\mathscr{F}^{\mathrm{RSF}}(C, f_1, f_2) = \sum_{i=1}^{2} \lambda_i \int \Big(\int_{\Omega_i} K_\sigma(x - y) |I(y) - f_i(x)|^2 \mathrm{d}y \Big) \mathrm{d}x + \upsilon \, |C| \,, \quad (3)$$

where $\Omega_1 = \mathrm{outside}(C)$, $\Omega_2 = \mathrm{inside}(C)$, and $f_1(x)$ and $f_2(x)$ are two values that approximate image intensities in Ω_1 and Ω_2, and K is a kernel function which is often chosen as a Gaussian kernel

$$K_\sigma(\boldsymbol{u}) = \frac{1}{(2\pi)^{n/2} \, \sigma^n} \mathrm{e}^{-|\boldsymbol{u}|^2/2\sigma^2} \quad (4)$$

with a scale parameter $\sigma > 0$. Li's model is able to handle inhomogeneous intensity, which is a big improvement.

In cell image segmentation, these models need adjusting because there are problems such as: 1) sometimes, we cannot properly segment the nucleolus from cytoplasts, as shown in Fig. 1, 2) the segmentation result depends greatly on the initialization of the level set function. Therefore, in the next part, we will describe the characteristics of the cell image and then propose our method for cell image segmentation.

2.2. Model of cell image segmentation

In practice, cells frequently have the following characteristics: the nucleolus is located inside the cytoplasm and the density of the nucleoli are bigger than that of cytoplasms. Therefore, a cell image has the following features: 1) the nucleolus image is located in the cytoplasm image, 2) the cytoplasm image is located in the background image , 3) the intensity of the nucleolus image is larger than that of the cytoplasm image, and 4) the intensity of the cytoplasm image is larger than that of the background image, as shown in Fig. 2. These features can be utilized in the segmentation processes. For example, we can make the ultimate level set function of background and nucleoli negative and the other part positive to segment the cell image. If the image does not satisfy 1) and 2) like Fig. 2(c), usually one level set function is not enough.

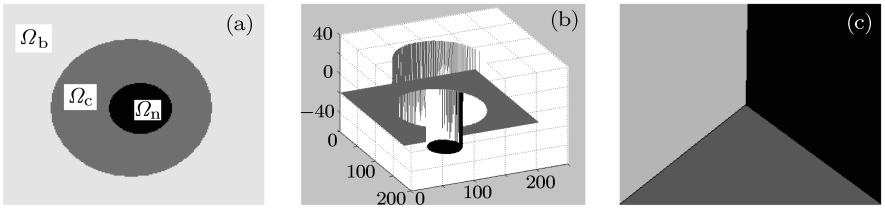


Fig. 2. (a) Original cell image; (b) ideal level set function where the nucleolus and background parts are negative and the cytoplasm part is positive or exactly the reverse; (c) other image.

Let Ω_b and I_b be the area and the intensity of the background, Ω_n and I_n be the areas of the nucleoli, Ω_c and I_c be the areas of cytoplasm. The cell image characteristics can be described as follows:

$$\Omega_n \subset \Omega_c \subset \Omega_b, \tag{5}$$

$$I_n > I_c > I_b. \tag{6}$$

In practice, we can statistically estimate the intensity range of the cell nucleoli image. Combining the initialization, we can add an item in order modify the energy functional

$$\mathscr{F}^{CS}(C, f_1, f_2) = \sum_{i=1}^{2} \lambda_i \int \left(\int_{\Omega_i} K_\sigma(x-y)|I(y) - f_i(x)|^2 \mathrm{d}y \right) \mathrm{d}x + \upsilon |C| + \eta \int_{\Omega_1} \|I(x) - R_c\|^2 \mathrm{d}x, \tag{7}$$

where R_c represents the approximate cytoplasm intensity range obtained by a priori knowledge and $\|I(y) - R_c\|$ represents the distance between the image intensity and R_c, and η is the coefficient of the item. Suppose $R_c = [R_{min}, R_{max}]$, we define $\|I(y) - R_c\|$ as

$$\|I(x) - R_c\| = \begin{cases} I(x) - R_{max}, & \text{if } I(x) > R_{max}, \\ 0 & \text{if } R_{max} > I(x) > R_{min}, \\ R_{min} - I(x), & \text{if } R_{min} > I(x). \end{cases} \tag{8}$$

If $I(x)$ is in the range of R_c, $\|I(x) - R_c\|$ equals zero. In particular, we use Ω_1 to represent all the pixels located in Ω_c but not in Ω_n and designate Ω_2 to the area in which the pixels are not located in Ω_1, i.e.

$$\Omega_1 = \Omega_c - \Omega_n, \quad \Omega_2 = \Omega_b - \Omega_1. \tag{9}$$

Our goal is to find out Ω_1. If we can achieve this, according to expression (5), we can easily obtain Ω_c and Ω_n, so only one level set function is enough to distinguish all three phases of the cell images. As we will show in the next section, by combining the initialization of the level set function, we can make it work in practice.

The last item mainly perishes the background and the nucleoli from the cytoplasm area, and speeds up convergence by preventing the level set function from frequently jolting from positive and negative values. For example, in the condition of Fig. 1(d), the function of the last item is to distinguish the nucleoli from cytoplasm that have not segmented properly. Through Eq. (7), we can also figure out the background from the cytoplasm because other parts of functional (7) remain the same as those from the RSF model detailed in Ref. [7].

3. Variational level set formulation of curve evolution

3.1. Level set formulation

In the level set method,[3] a contour $C \subset \Omega$ is indicated by the zero level set of the Lipschitz function $\phi : \Omega \to R$, which is called a level set function. In this paper, we let the level set function ϕ take positive and negative values outside and inside the contour C, respectively. Ideally, we hope that ϕ takes positive values in Ω_1 and negative values in Ω_2. Let H be the Heaviside function, the energy functional (7) can be expressed as

$$\mathscr{F}^{\mathrm{CS}}(\phi, f_1, f_2) = \sum_{i=1}^{2} \lambda_i \int \left(\int K_\sigma(x-y) \left| I(y) - f_i(x) \right|^2 M_i(\phi(x)) \mathrm{d}y \right) \mathrm{d}x + \upsilon \int \left| \nabla H(\phi(x)) \right| \mathrm{d}x + \eta \int \left\| I(x) - R_{\mathrm{c}} \right\|^2 H(\phi(x)) \mathrm{d}x, \tag{10}$$

where $M_1(\phi) = H(\phi)$, $M_2(\phi) = 1 - H(\phi)$, $\int \left| \nabla H(\phi(x)) \right| \mathrm{d}x$ is the length of the zero level contour of ϕ and $\int \left\| I(x) - R_{\mathrm{c}} \right\|^2 H(\phi(x)) \mathrm{d}x$ is the total sum of all pixel distances from the intensity and the estimated intensity range of the cytoplasm. Note that this length term is commonly used in variational level set methods for the regularization of the zero level contour.[4,5] The length of the zero level contour can be equivalently expressed as the integral $\int \delta(\phi) \left| \nabla(\phi) \right| \mathrm{d}x$ with the Dirac delta function δ, which is often used in variational level set methods.[19]

In practice, the Heaviside function H in the above energy functional is approximated by a smooth function H_ε defined as

$$H_\varepsilon(x) = \frac{1}{2} \left[1 + \frac{2}{\pi} \arctan\left(\frac{x}{\pi} \right) \right]. \tag{11}$$

The derivative of H_ε is

$$\delta_\varepsilon(x) = H'_\varepsilon(x) = \frac{1}{\pi} \frac{\varepsilon}{\varepsilon^2 + x^2}. \tag{12}$$

By replacing H with H_ε, the energy functional $\mathscr{F}^{\mathrm{CS}}$ in Eq. (10) is then approximated as follows:

$$\mathscr{F}_\varepsilon^{\mathrm{CS}}(\phi, f_1, f_2) = \sum_{i=1}^{2} \lambda_i \int \left(\int K_\sigma(x-y) \left| I(y) - f_i(x) \right|^2 M_i^\varepsilon(\phi(x)) \mathrm{d}y \right) \mathrm{d}x + \upsilon \int \left| \nabla H_\varepsilon(\phi(x)) \right| \mathrm{d}x + \eta \int \left\| I(x) - R_{\mathrm{c}} \right\|^2 H_\varepsilon(\phi(x)) \mathrm{d}x, \tag{13}$$

where $M_1^\varepsilon(\phi) = H(\phi)$ and $M_2^\varepsilon(\phi) = 1 - H(\phi)$.

To accelerate the calculation progress, we add an item proposed by Li[19] to Eq. (13), the ultimate function then becomes

$$\mathscr{F}_\varepsilon^{\mathrm{CSM}}(\phi, f_1, f_2) = \sum_{i=1}^{2} \lambda_i \int \left(\int K_\sigma(x-y) \left| I(y) - f_i(x) \right|^2 M_i^\varepsilon(\phi(x)) \mathrm{d}y \right) \mathrm{d}x + \upsilon \int \left| \nabla H_\varepsilon(\phi(x)) \right| \mathrm{d}x + \eta \int \left\| I(x) - R_{\mathrm{c}} \right\|^2 H_\varepsilon(\phi(x)) \mathrm{d}x + \mu \int \frac{1}{2} (|\nabla \phi(x)| - 1)^2 \mathrm{d}x, \tag{14}$$

where μ is a positive constant. To minimize expression (14), its gradient flow is used as the level set evolution equation in the proposed method.

3.2. Energy minimization

Here, we use the standard gradient descent method to minimize the energy functional (14) and use $\partial \mathscr{F} / \partial \phi$ to represent the Gateaux derivative of functional $\mathscr{F}$, so the following evolution equation:

$$\frac{\partial \phi}{\partial t} = -\frac{\partial \mathscr{F}}{\partial \phi} \tag{15}$$

is the gradient flow that minimizes the functional $\mathscr{F}$. For a particular functional $\mathscr{F}(\phi)$ defined explicitly in terms of ϕ, the Gateaux derivative can be computed and expressed in terms of the function ϕ and its derivatives.

From Ref. [7], we know that for a fixed level set function ϕ, we can minimize the functional $\mathscr{F}_\varepsilon^{\mathrm{CSM}}(\phi, f_1, f_2)$ in Eq. (15) using the following functions $f_1(x)$ and $f_2(x)$:

$$f_i(x) = \frac{K_\sigma(x) * [M_i^\varepsilon(\phi(x)) I(x)]}{K_\sigma(x) * M_i^\varepsilon(\phi(x))}, \quad i = 1, 2. \tag{16}$$

Keeping f_1 and f_2 fixed, we minimize the energy functional $\mathscr{F}_\varepsilon^{\mathrm{CSM}}(\phi, f_1, f_2)$ with respect to ϕ using the standard gradient descent method by solving the gra-

dient flow equation as follows:

$$\frac{\partial \phi}{\partial t} = -\delta_\varepsilon(\phi)(\lambda_1 e_1 - \lambda_2 e_2) + \upsilon \delta_\varepsilon(\phi)\mathrm{div}\left(\frac{\nabla \phi}{|\nabla \phi|}\right) + \mu\left(\nabla^2\phi - \mathrm{div}\left(\frac{\nabla \phi}{|\nabla \phi|}\right)\right) - \eta\delta_\varepsilon(\phi)\left\|I(x) - R_\mathrm{c}\right\|^2, \quad (17)$$

where δ_ε is the smoothed Dirac delta function given by expression (12), and e_1 and e_2 are the functions

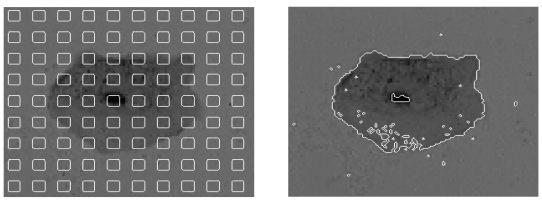
$$e_i(x) = \int K_\sigma(y-x)\left|I(x) - f_i(y)\right|^2 \mathrm{d}y, \quad i = 1, 2, \quad (18)$$

where f_1 and f_2 are given by expression (16).

The above expression (17) is the level set evolution equation to be solved in the proposed method. The first term on the right-hand side is referred to as a data fitting term and is responsible for driving the active contour towards object boundaries. The second term has an arc smoothing effect on the contour to maintain the regularity of the contour. The third term is named by Li as a level set regularization term, which serves to maintain the regularity of the level set function. The final term we add here has the function of eliminating the background and nucleoli from the cytoplasm area.

3.3. Initialization with OTSU

Theoretically, the initial level set function can be in any form without limitation. The most familiar initial zero level set is as shown in Fig. 3(a).



(a) (b)

Fig. 3. Initial level set functions: panel (a) is for the most familiar case, panel (b) is for cases where OSTU is used to initialize the function.

However, in practice, the initial zero level set has great influence on the segmentation result. In many cases, an inappropriate initial value may even cause the ultimate result to convert into a local optimal solution, as shown in Fig. 1(b).

In this article, a priori judgment has been used to set the initial level set function. We first calculated the intensity arrangement of the cytoplasm and the background using OTSU method and we utilized a priori knowledge to set the intensity arrangement of the nucleolus. Finally, we used the intensity arrangement to set the initial level set function: the estimated cytoplasm parts with positive values and other parts with negative values. This could speed up the calculation and avoid a local optimal solution.

4. Results and discussion

The proposed method has been tested with synthetic and real cell images. Unless otherwise specified, we use the following parameters in this paper: $\sigma = 3.0$, $\lambda_1 = \lambda_2 = 1.0$, time step $\Delta t = 0.1$, $\mu = 1$, and $\upsilon = 0.010 \times 255 \times 255$. As described in Ref. [7], small scale σ produces a more accurate location of the object boundary, while it is more independent of the location of the initial contour when a larger σ is used. λ_1 and λ_2 are positive coefficients of power, one point belonging to two parts and often set to be equal to 1.0. Δt is the time step used to control the evolution speed of the level set function and is often set to be 0.1 according to the magnitude of level set function. $\mu = 1$ means that we want to keep the angle between the level set function and the horizontal direction at 45°. And υ is the coefficient of the length of curve and often set to match the area exponentially.

We first show the results for a synthetic cell image 193×162 in size in Fig. 4 and then show real cell images in Figs. 5 and 6. The first row of Fig. 4 is for the case using previous model. Column (a) is for the traditional original level set function shapes, column (b) is for the states after 5 iterations, column (c) is for the case after 10 iterations, column (d) is for the zero level set after 150 iterations and column (e) is for the mesh of the final level set function. The average iteration time is about 0.10648 s. All experiments were performed using a hp workstation xw8200 with Xeon(TM) 3.40 GHz cpu and 3.00 GB memory, the software used is Microsoft Windows XP Service Pack 2 plus Matlab7.6.0. The second row of Fig. 4 is for the case where OTSU is used to segment the cell from its backgrounds, column (b) is for the scenario after 5 iterations, column (c) is for the scenario after 8 iterations, and column (d) is for the case after 16 iterations, the function is stabilized after 16 iterations, each iteration takes 0.098 s. In the third row, we use OSTU to first segment the nucleolus and cytoplasm from their relative backgrounds, column (b) is for the case after 6 iterations, column (c) is for the scenario after 8 iterations, and (d) is for the stabilized case after 11 iterations. Each iteration takes about 0.094 s.

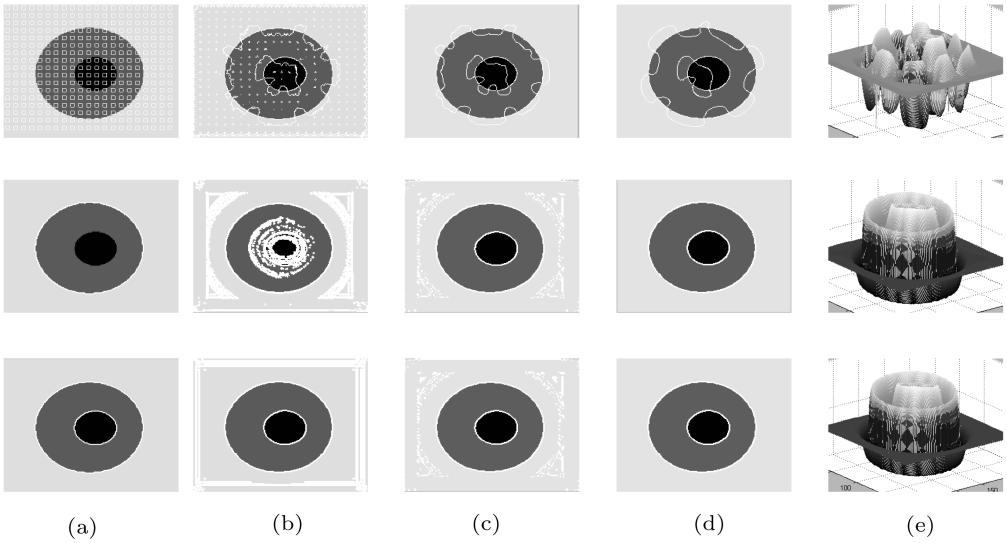


Fig. 4. Synthetic cell images segmented using different initial level set functions.

Figure 5 shows the segmentation process of a real cell image containing only one cell, with the original size of the picture being 101×90. The first row illustrates the traditional initial level set functions in which the level set function is stabilized after 16 iterations, but fails to segment the cytoplasm from the background. The second row shows the results obtained with our method, showing the level set function stabilized after 10 iterations and the segmented cytoplasm and nucleolus from their relevant backgrounds.

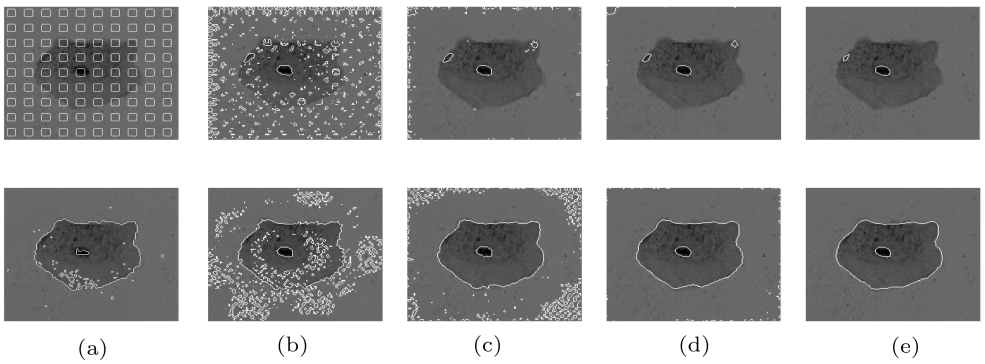


Fig. 5. Real cell image segmented using different initial level set functions.

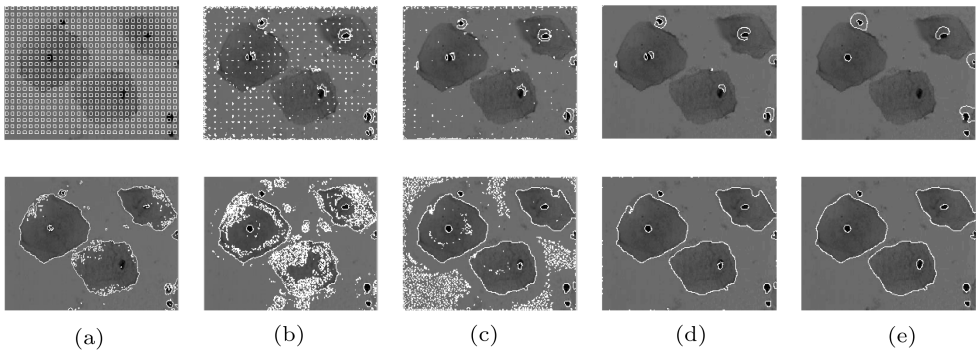


Fig. 6. Real cell image segmenting process.

Figure 6 shows the segmentation process of a real cell image with several different shaped cells in it, the original size of the picture is 292×218. The first row illustrates the traditional initial level set functions in which the level set function is stabilized after 40 iterations, but fails to segment the cytoplasm from the background. The second row shows the results obtained with our method, showing the level set function from being stabilized after 18 iterations, and the segmented cytoplasm and nucleolus from their relevant backgrounds.

As illustrated by the previous section, previous models could not handle the cell image segmentation very well without modification. It often falls into the traps of local optimal solution and is very sensitive to many parameters. In our method, the final segmentation is very "near" to the coarsely segmented result using the OSTU algorithm, so our method is insensitive to parameters and speeds up the segmentation process.

Our method primarily needs 2 additional calculations, one is to use OSTU to compute the rough values for the nucleoli, cytoplasm and background, and the other is to calculate $-\eta\delta_\varepsilon(\phi)\left\|I(x)-R_{\mathrm{c}}\right\|^2$. These steps take a short time and help a great deal to speed up the convergence of segmentation.

The item $-\eta\delta_\varepsilon(\phi)\left\|I(x)-R_{\mathrm{c}}\right\|^2$ mainly prevents the level set function "turning over" from one end to another. This helps us to segment 3 phases by using one level set. In the meantime, in the experiment we find that this item slightly speeds up the convergence process because it points towards the convergence direction.

On the other hand, we find that the time consumed by each iteration has no notable difference among models. When the size grows, the burden augments remarkably. This subject needs further study in the future.

References

[1] Lian L J and Ling Q Z 2006 *Gynecologic Oncology* (Beijing: People's Medical Publishing House) p. 289 (in Chinese)

[2] John L Semmlow 2004 *Biosignal and Biomedical Image Processing* (New York: Marcel Derkker, Inc) p. 343

[3] Stanley Osher and James A Sethian 1988 *J. Comput. Phys.* **79** 12

[4] Tony Chan and Luminita Vese 2001 *IEEE Trans. Image Processing* **10** 266

[5] Luminita Vese and Tony Chan 2002 *Int. J. Comput Vis.* **50** 271

[6] Zhao G Z 2010 *Chin. Phys.* B **19** 070203

[7] Li C M 2008 *IEEE Trans. Image Processing* **17** 1940

[8] Caselles V 1997 *Int. J. Comput. Vis.* **22** 61

[9] Kass M 1987 *Int. J. Comput. Vis.* **1** 321

[10] Kichenassamy S 1995 *Proc. 5th Int. Conf. Comput. Vis.* **8** 10

[11] Kimmel R 1995 *IEEEE Trans. Pattern Anal. Match. Intell.* **17** 635

[12] Vasilevskiy A 2002 *IEEE Trans. Pattern Anal. Mach. Intell.* **24** 1565

[13] Paragios N 2002 *Int. J. Comput. Vis.* **46** 223

[14] Ronfard R 1994 *Int. J. Comput. Vis.* **13** 229

[15] Samson C 2000 *IEEE Trans. Patt. Anal. Mach. Intell.* **22** 460

[16] Duan C J 2009 *J. Software* **20** 1106

[17] Zhang K H 2010 *Image and Vision Computing* **28** 668

[18] Siddhartha Bhattacharyya 2011 *Appl. Soft. Computing* **11** 946

[19] Li C M 2005 *Proc. IEEE. Conf. Comput. Vision and Pattern Recognition* **1** 430

[20] Li C M 2007 *CVPR* 1

[21] Mumford D and Shah J 1989 *Commun. Pure Appl. Math.* **42** 577